

AD-A242 379

DTIC
ELECTE
NOV 12 1991

*Original contains color plates. All DTIC reproductions will be in black and white.

91-15455

Best Available Copy

ADMIRALTY RESEARCH ESTABLISHMENT
Procurement Executive Ministry of Defence
Hastings GOSPORT Hants PO12 2AG

91 1112 089

UNLIMITED

DEFINITION STATEMENT A

Approved for public release:
Distribution is unlimited

0085672

CONDITIONS OF RELEASE

BR-113198

DRIC U

COPYRIGHT (c)
1988
CONTROLLER
HMSO LONDON

DRIC Y

Reports quoted are not necessarily available to members of the public or to commercial organisations.

UNCLASSIFIED

ARE TM(UHU) 88305

June 1988

ANALYSIS OF EXPERIMENTS TO MEASURE
BODY VORTICES IN CURVED FLOW

(U)

BY

B Ward
A R J M Lloyd

Summary

This Technical Memorandum describes the methods used to fair data on vortices shed from a body in curved flow. The methods used to calculate local circulation density, total circulation density, apparent centre of total circulation, local vortex centre and local vortex core radius are described and empirical equations to represent the results are given.

© British Crown Copyright 1991/MOD

Published with the permission of the
Controller of Her Britannic Majesty's
Stationery Office

Admiralty Research Establishment
Haslar Gosport Hants PO12 2AG

©
Copyright
Controller HMSO London
1988

UNCLASSIFIED

Contents

	Page
Notation.	iii
1. Introduction.	1
2. Vorticity; Some Background Reading.	1
3. The Experiment.	4
4. Typical Data Set.	6
5. Data Analysis Program.	7
6. Empirical Equations to Represent the Results.	24
7. Conclusions.	28
References.	30

Accession For	
NTIS GRA&I	<input checked="" type="checkbox"/>
DTIC TAB	<input type="checkbox"/>
Unannounced	<input type="checkbox"/>
Justification	
By _____	
Distribution/	
Availability Codes	
Dist	Avail and/or Special
A-1	

Notation		
α	Angle of incidence	deg
Γ	Circulation	m ² /sec
Γ_θ	Circulation density at a given angle	m ² /sec/rad
θ	Angle of strut	deg or radians
θ_0	Separation angle	deg or radians
θ_{BV}	Centre of total circulation - angular position	deg or radians
ζ	Vorticity	rad/sec
ζ_{MAX}	Maximum vorticity	rad/sec
$a_0, b_1, c_2, d_3 \dots$	Coefficients in empirical equations	various
D	Body diameter	metres
L	Length of body	metres
q	Induced velocity at radius R_v from vortex centre	metres/sec
r	Radius from body axis to position of probe	metres
r_*	Local vortex core radius (radius for maximum induced velocity)	metres
r'	Non-dimensional rate of turn or turn parameter; L/S	
R	Local radius of body	metres
R_1	Centre of local vortex - radial position	metres
R_{BV}	Centre of total circulation - radial position	metres
R_v	Radius from the centre of the vortex	metres
R'_v	Non-dimensional radius from the centre of the vortex; R_v/r_*	
S	Arm radius; radius of turn	metres

u	Free stream velocity in the X direction	metres/sec
v	Velocity induced in Y direction	metres/sec
w	Velocity induced in Z direction	metres/sec
x	Longitudinal distance from nose of body; positive aft	metres
x'	Non-dimensional distance from nose to body; x/L	
X	axis which the vortex lies along	
Y	} Transverse Planes	
Z		

ANALYSIS OF EXPERIMENTS TO MEASURE
BODY VORTICES IN CURVED FLOW

By B Ward
A R J M Lloyd

1. INTRODUCTION

Experiments on the Rotating Arm in the Manoeuvring Tank at ARE(H) provided data on vortices shed from a body of revolution in curved flow. The experiments in support of SUBSIM (Reference 1) took place during 1986 (Reference 2) and 1987 (Reference 3). Reference 4 also gives an extensive discussion of these experiments. This memorandum describes a detailed analysis of the experiment results.

2. VORITICITY; SOME BACKGROUND READING

2.1. Characteristics of Vortices (See Reference 4)

A vortex is shown in Figure 1 with the free stream velocity u in the X direction. Velocities v and w are induced in Y, Z directions respectively. At a radius $R_v = \sqrt{Y^2 + Z^2}$ metres from the centre of the vortex a velocity $q = \sqrt{v^2 + w^2}$ is induced (see Figure 2a). From classical potential theory $q = \Gamma / 2\pi R_v$ metres/sec which leads to infinite induced velocity and shear at the origin as shown in Figure 2b.

In reality viscous effects stop these large velocities from occurring. It is assumed that the central area of the vortex rotates more or less as a solid core with the induced velocity close to the centre increasing linearly with the radial distance from the centre. This is simulated by the modified equation

$$q = \frac{\Gamma}{2\pi R_v} \left[1 - \exp \left[- 1.26 R_v'^2 \right] \right] \text{ metres/second}$$

where

$$R_v' = R_v / r_*$$

and r_* is the core radius of the viscous vortex (defined as the radius at which the induced velocity q is a maximum).

Here the induced velocity is reduced to zero at the centre but reaches its inviscid value at large distances from the centre.

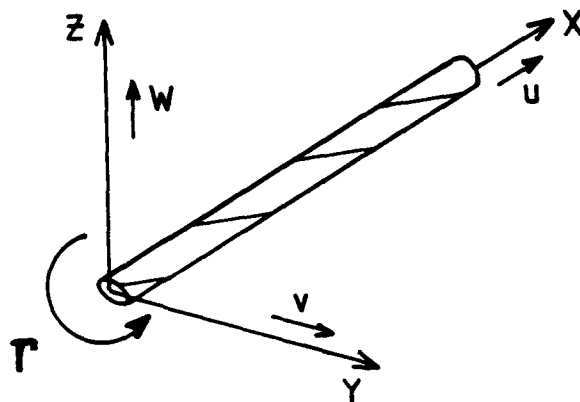


Figure 1

VORTEX NOTATION

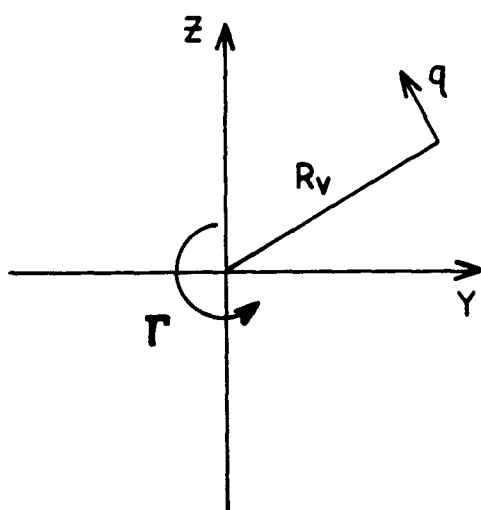


Figure 2a

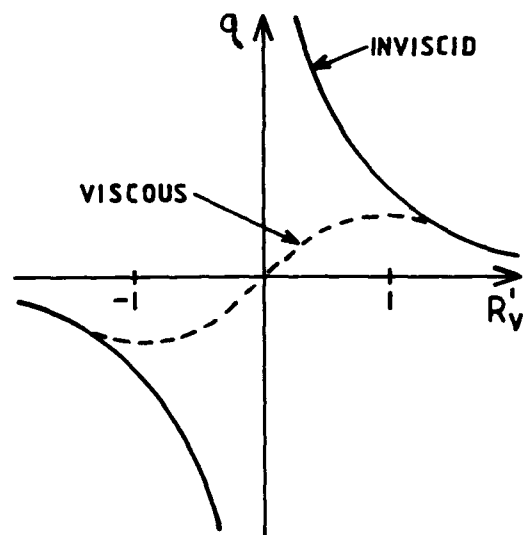


Figure 2b

VORTEX FORMULATIONS

2.2. Body Vortices

If the body is at a moderate angle of incidence and turn rate the boundary layer on the leeward surface separates as shown in Figure 3. The location of the separation line may be quantified in terms of the 'separation angle' θ_0 . Vorticity shed from the boundary layer is convected away and coalesces to form a diffuse pair of vortices with cores almost parallel to the body axis. The vortices' strength increases towards the tail of the body as more vorticity is added.

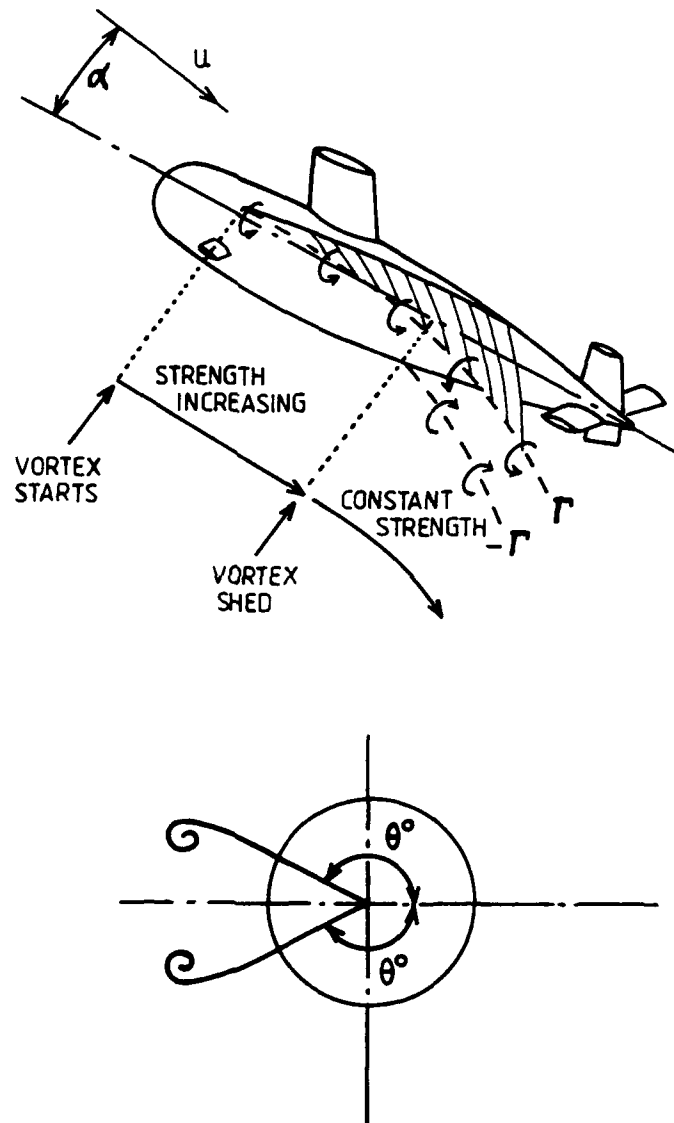


Figure 3

BODY VORTEX

3. THE EXPERIMENT

A 5.0 metre long model body of revolution was attached to the Rotating Arm as shown in Figure 4a.

Table 1 gives the model dimensions.

Table 1

MODEL DIMENSIONS (LENGTH, 5 m; MAXIMUM RADIUS, 0.294 m)

x'	R (m)
0	0
0.05	0.206
0.10	0.266
0.15	0.291
0.20-0.65	0.294
0.70	0.289
0.75	0.274
0.80	0.247
0.85	0.206
0.90	0.151
0.95	0.084
1.00	0

A Freestone vorticity probe (Reference 5) was designed and built with a radius of 10 mm. The probe was attached to a strut which was built to provide measurements out to a radius of 1.5 x body diameter. An inclinometer was used to set up the strut such that in the position referred to as $\theta = 90$ degrees it protruded vertically from the top of the body and at $\theta = 0$ degrees it was horizontal on the inboard side of the model, (see Figure 4b).

Three different strut-body stations were used in the test conditions (a) $x' = 0.925$, (b) $x' = 0.85$, (c) $x' = 0.7$ where $x' = x/L$ (see Figure 4b).

Incidence angle α was set with the nose towards the centre of the arm (see Figure 4c).

The probe was traversed from close to the body surface to the limits of the strut where the vorticity was expected to be zero. This was done with the strut at angles of 0, 10, 20, ... 90 degrees. The arm was rotated counter-clockwise. The non-dimensional rate of turn or turn parameter r' was varied by changing the arm radius S . About 130 data readings were obtained for each test condition.

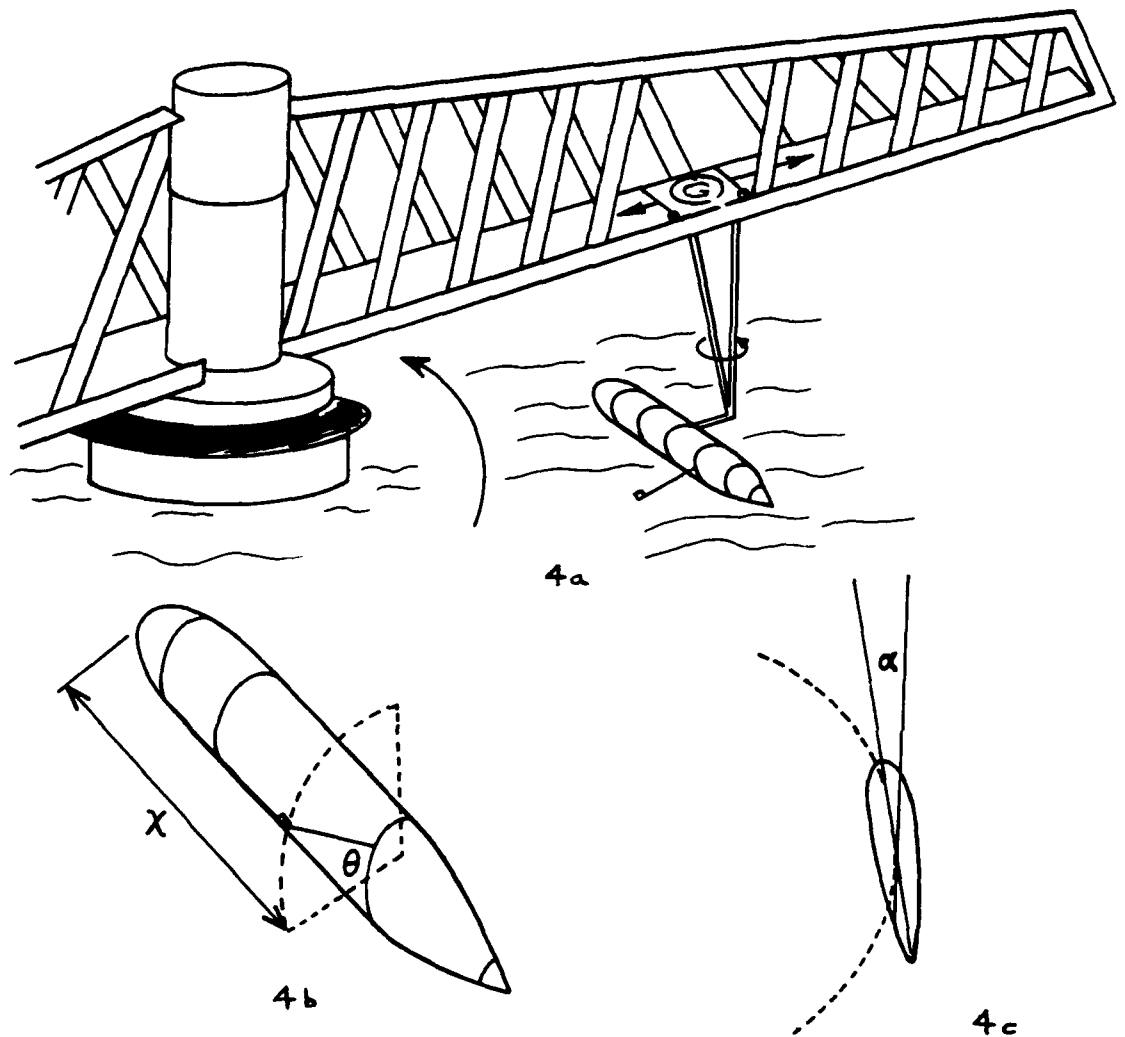


Figure 4

THE EXPERIMENT

4. TYPICAL DATA SET

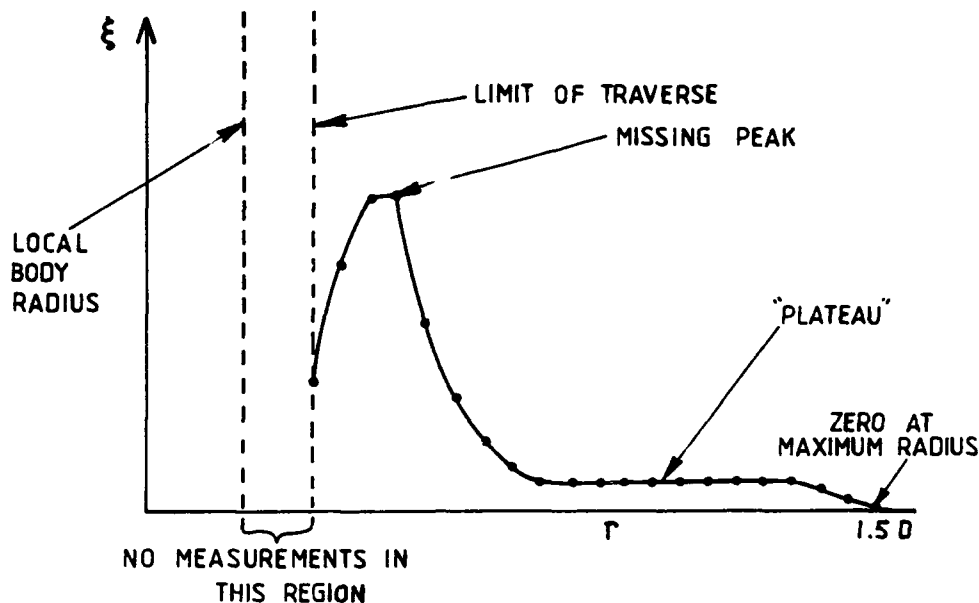


Figure 5

TYPICAL VORTICITY TRAVERSE

Figure 5 shows a sketch of a typical vorticity traverse (plot of vorticity versus radius for a given angle θ). A number of salient features are apparent;

- a. The peak value has probably been missed due to the limited number of data values.
- b. The physical dimensions of the probe precluded any measurements close to the local body surface.
- c. The traverses appear to come down to a 'plateau' as the radius increases, whereas it would have been expected that they would decrease smoothly to zero at the 'edge' of the vortical flow. This is probably associated with zero errors in the Freestone probe. It was found in Reference 2 that the probe gave small levels of 'vorticity' in uniform flow when no vorticity was expected and that these zero errors were functions of the flow direction at the probe. A simple correction was devised based on the results obtained at the outer limits of the strut, and this was applied to each traverse, forcing the vorticity at $r = 1.5 \times D$ to be zero. However, the flow direction changes as the probe is moved towards the body and this will affect the zero error correction. No simple method of quantifying this effect has been devised.

To overcome these shortcomings the data were faired to a more expected form and ensuring smooth variations as each of the parameters was varied. This involved;

- a. Inserting estimated additional points close to the local radius of the body.
- b. Interpolating extra points throughout the curve including, at times, a point for peak vorticity.
- c. Bringing traverses down to zero at the apparent edge of the vortical flow.
- d. Ensuring that the estimated peak vorticity increased smoothly with strut angle.

5. DATA ANALYSIS PROGRAM

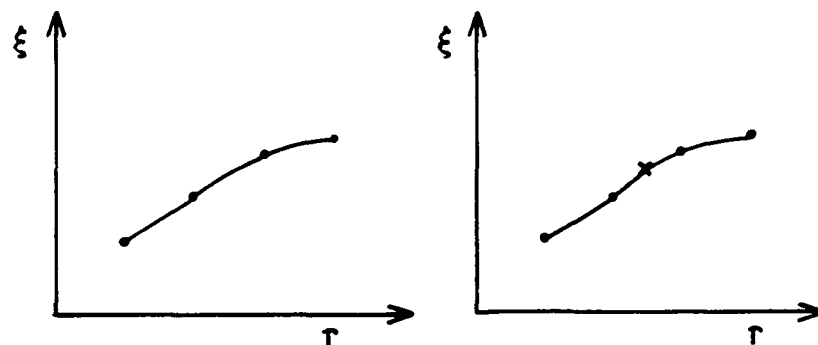
5.1. Introduction

A FORTRAN program entitled INTERP was developed on the ARE(H) PRIME 9955 Computer to fair the data. The fairing involved human judgement in altering and inserting data points depending on the trend of the curve and the expected behaviour of the traverses.

The program used the GINO graphics package which enabled plots of vorticity traverses to be displayed on the VDU, analysed, subsequently altered and analysed further.

5.2. Interpolating Extra Data Points

Each vorticity traverse ($\theta = 10$ degrees to 90 degrees) was analysed. When it was considered appropriate cubic polynomials were calculated to fit all sets of four adjacent points (1,2,3,4), (2,3,4,5) etc, for the particular angle under examination. This involved taking the four points (Figure 6) deriving a system of equations and then solving them. The resulting cubic polynomial $\zeta(r) = a_3r^3 + a_2r^2 + a_1r + a_0$ was used to calculate an additional point between the middle two points, (Figure 7).



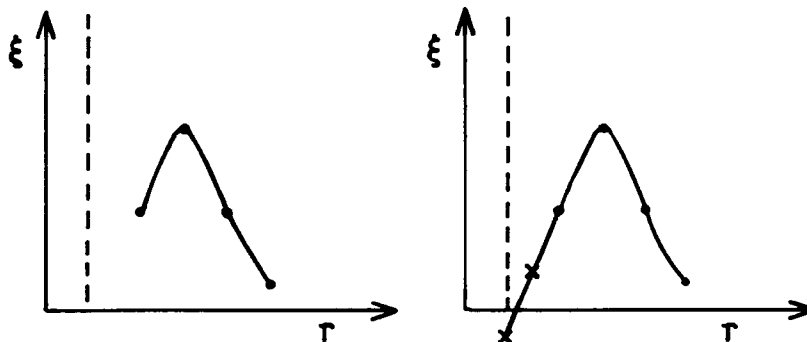
Figures 6 and 7

INTERPOLATION OF EXTRA POINT

Doing so throughout the curve, $N-3$ extra points were interpolated (where N is the total number of original data points). These extra points ensured a more accurate numerical integration and in certain cases a more reasonable peak value for vorticity was achieved.

5.3. Additional Points Close to the Body Surface

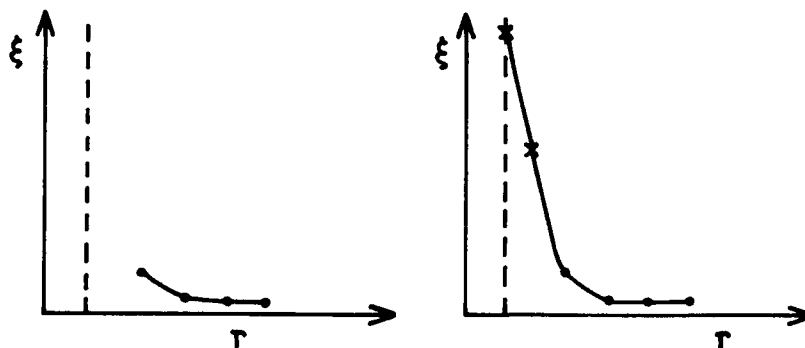
Figures 8 and 9 show how a traverse for a strut angle of, say 30 degrees, was extrapolated to the body surface. In this example the trend of the curve shown implies that the vorticity is negative at the body surface.



Figures 8 and 9

EXTRAPOLATING EXTRA POINTS CLOSE TO BODY SURFACE FOR STRUT ANGLE $\theta \approx 30$ DEGREES

Figures 10 and 11 show how a traverse for a high strut angle of, say 90 degrees, was extrapolated to the body surface. At such a strut position it was assumed that the vorticity would peak at the body surface. Hence the trend of the curve will be as shown in Figure 11. The extrapolated maximum vorticity at the body surface at angles of 80 degrees and 90 degrees was subsequently reassessed by the method described in 5.5.

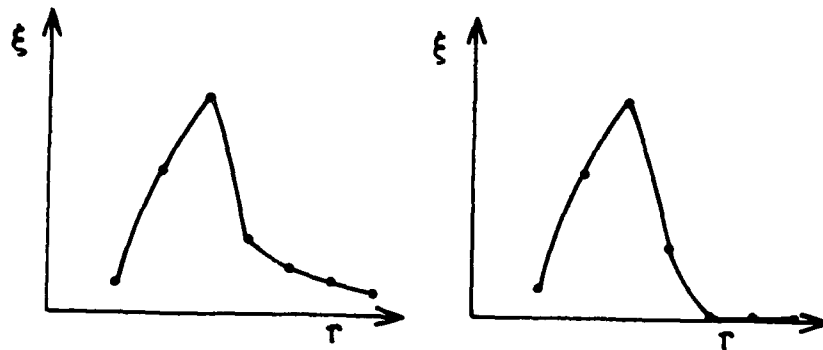


Figures 10 and 11

EXTRAPOLATING EXTRA POINTS CLOSE TO BODY SURFACE FOR STRUT ANGLE $\theta \approx 90$ DEGREES

5.4. Eliminating the Zero Plateau

The traverse was brought down to zero at the apparent outer edge of the vortical flow. No formal procedure was employed, but the gradient of the curve was used to estimate by eye where the traverse was brought to zero as shown in Figures 12 and 13. In general, the traverse was brought down more sharply at higher strut angles eg 80 degrees, 90 degrees.



Figures 12 and 13

ELIMINATING ZERO PLATEAU

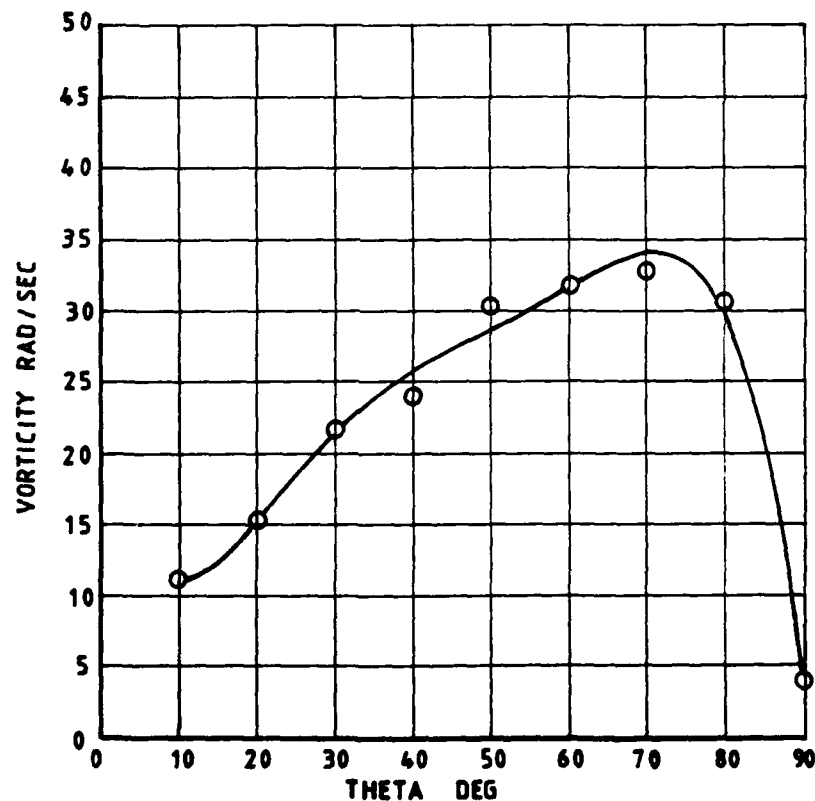


Figure 14

ESTIMATED PEAK VORTICITY ($x' = 0.925$, $r' = 0.3$, $\alpha = 7.5$ DEGREES)

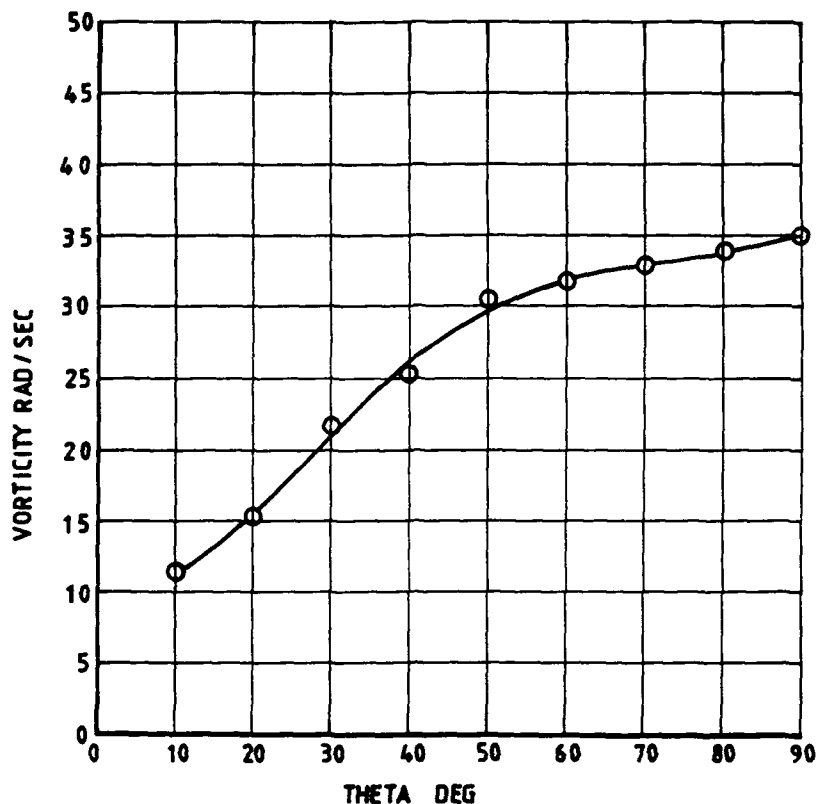


Figure 15

ADJUSTED VALUES OF PEAK VORTICITY
($x' = 0.925$, $r' = 0.3$, $\alpha = 7.5$ DEGREES)

5.5. Increasing the Peaks of Vorticity Traverses

A regression polynomial of the form $\zeta_{MAX} = b_0 + b_1\theta + b_2\theta^2 + b_3\theta^3 + b_4\theta^4 + b_5\theta^5$ was fitted to the estimated peak vorticity data for each test condition. An example is shown in Figure 14. It was argued that the peak vorticity should increase monotonically up to a maximum at about $\theta = 90$ degrees where the boundary layer separates from the body surface. If this is the case the estimated peak values at $\theta = 80$ degrees and 90 degrees are clearly too low. Recalling that these values were estimates based on extrapolation (as shown in Figures 10 and 11) it was considered justifiable to increase their values as shown in Figure 15.

The regression curve was used to assess whether any further adjustments to the estimated peak levels were required at other values of θ . In Figure 15 an example of such an adjustment can be seen for $\theta = 40$ degrees.

In certain cases these changes demanded reassessments of earlier decisions. In particular increasing the peak vorticity levels at high

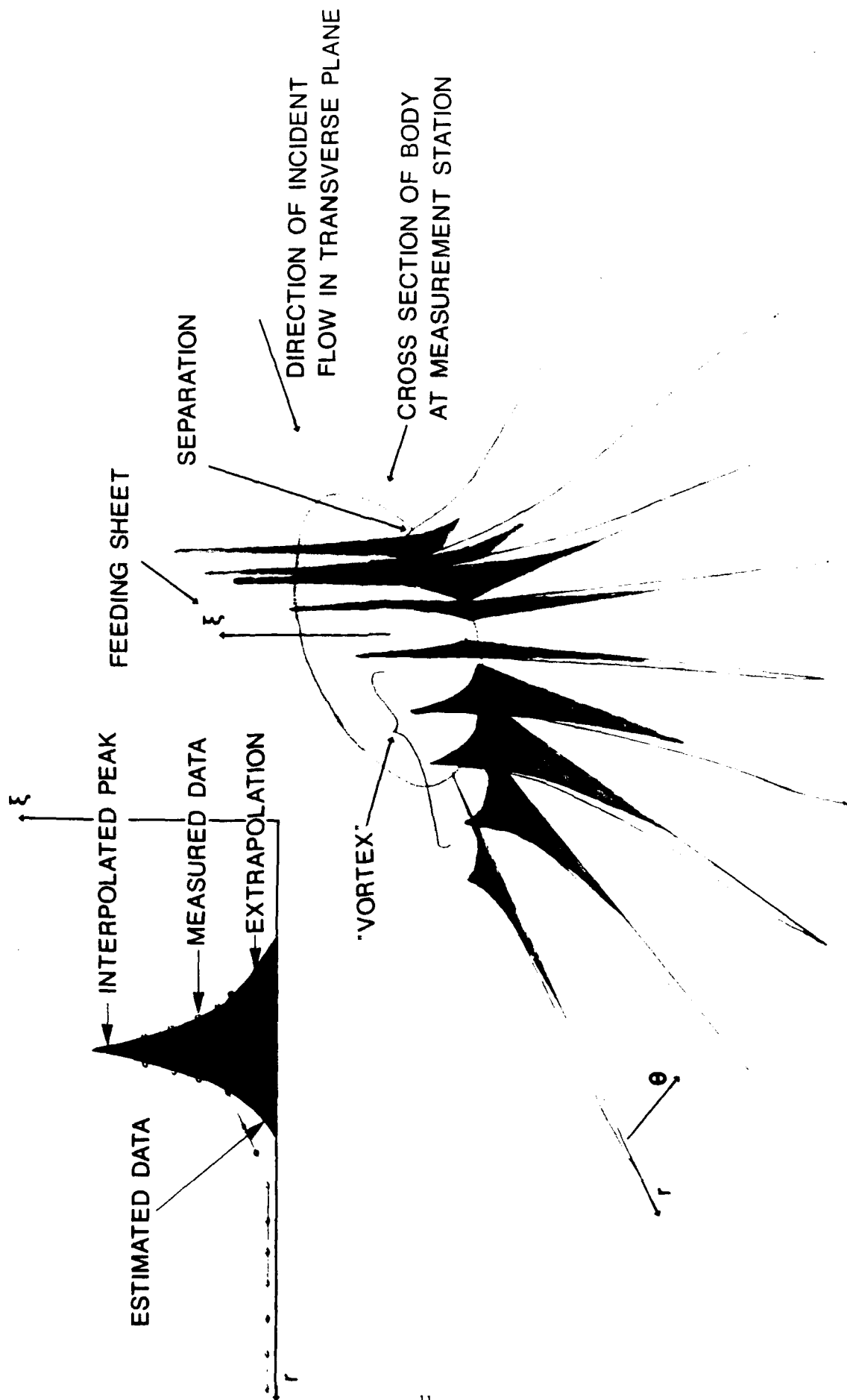


Figure 16

FAIRED VORTICITY TRAVERSES - AN ARTIST'S IMPRESSION

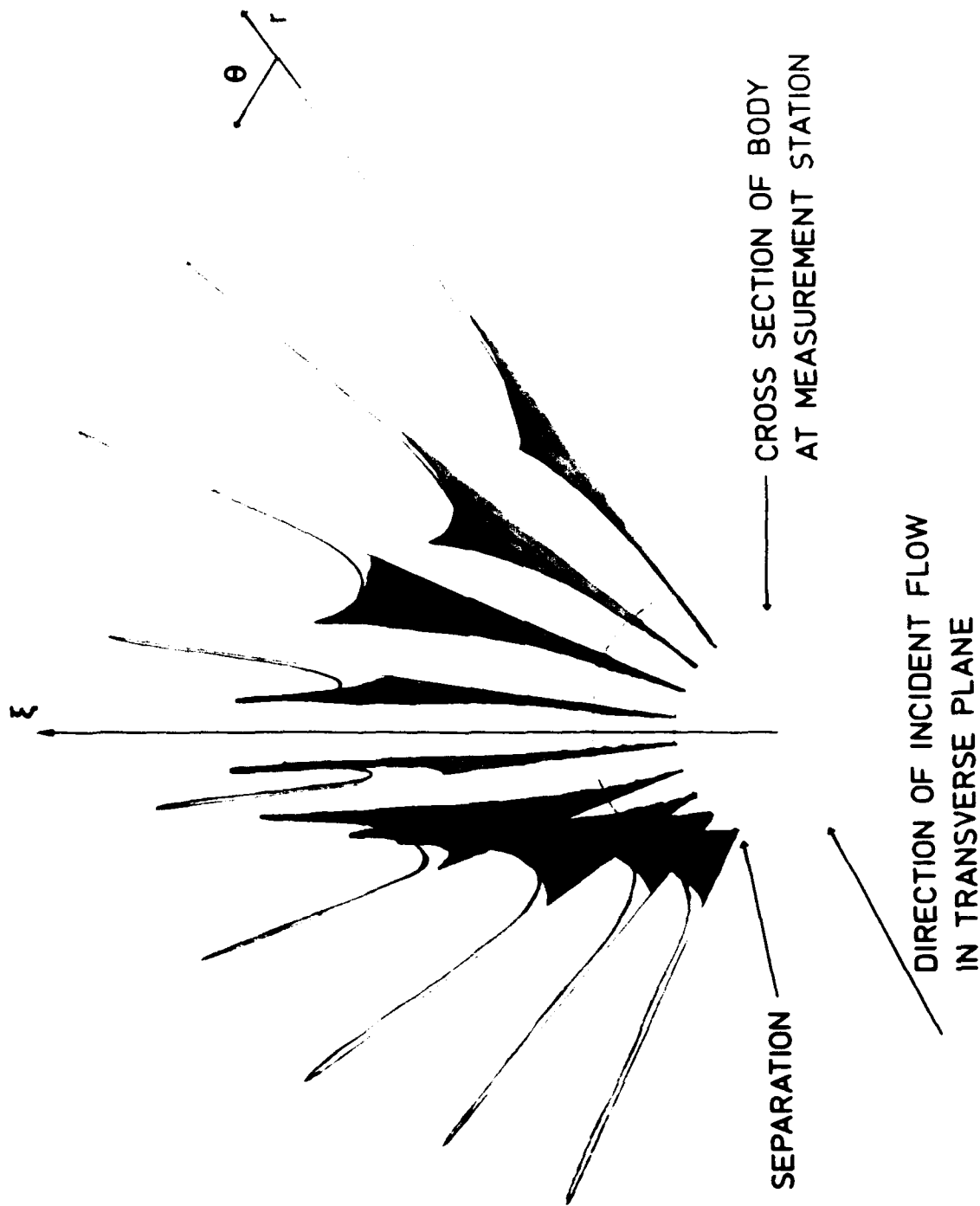


Figure 17
FAIRED VORTICITY TRAVERSES AN ARTIST'S IMPRESSION

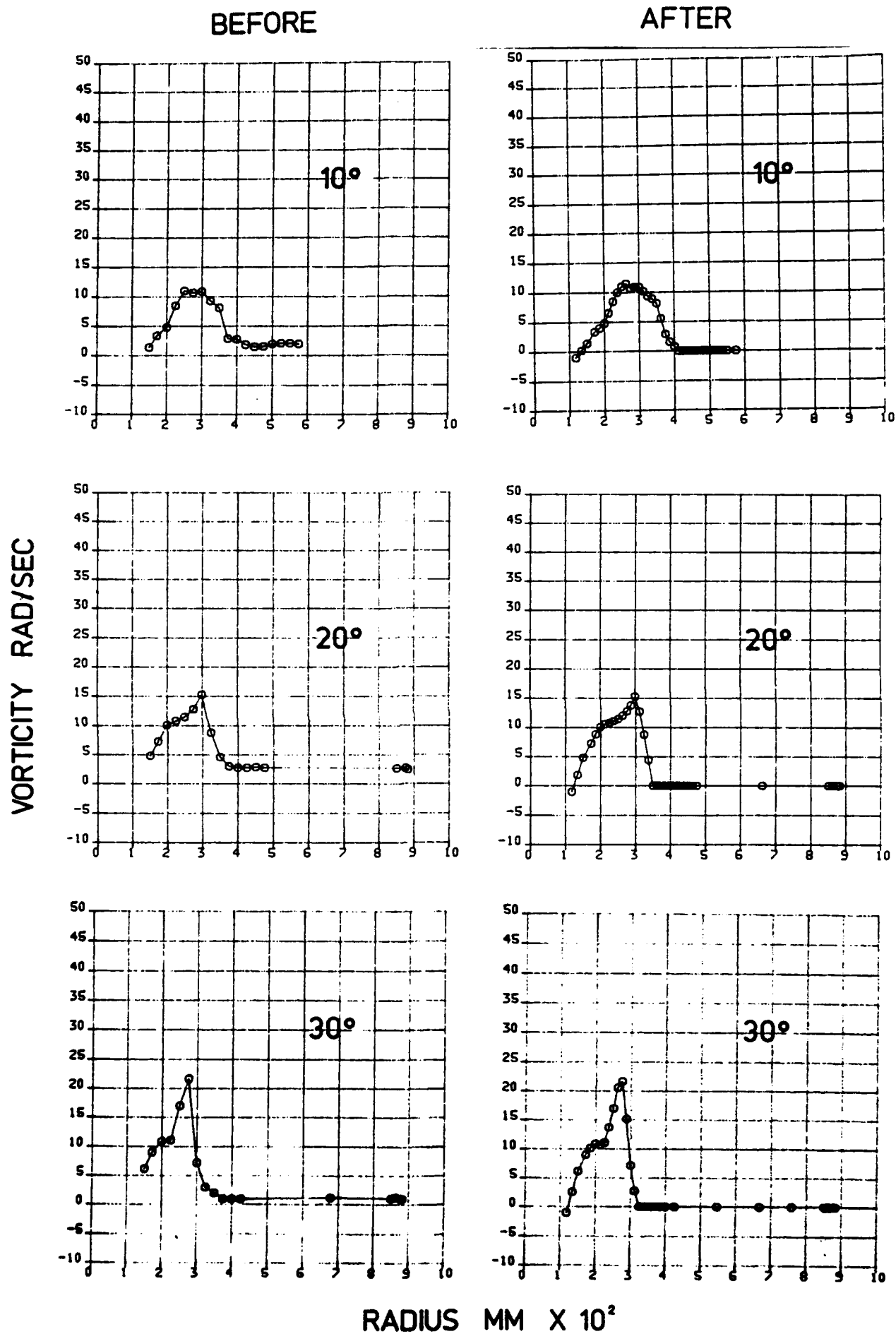


Figure 18a
VORTICITY TRAVERSES - BEFORE AND AFTER FAIRING
 ($x' = 0.925$, $r' = 0.3$, $\alpha = 7.5$)

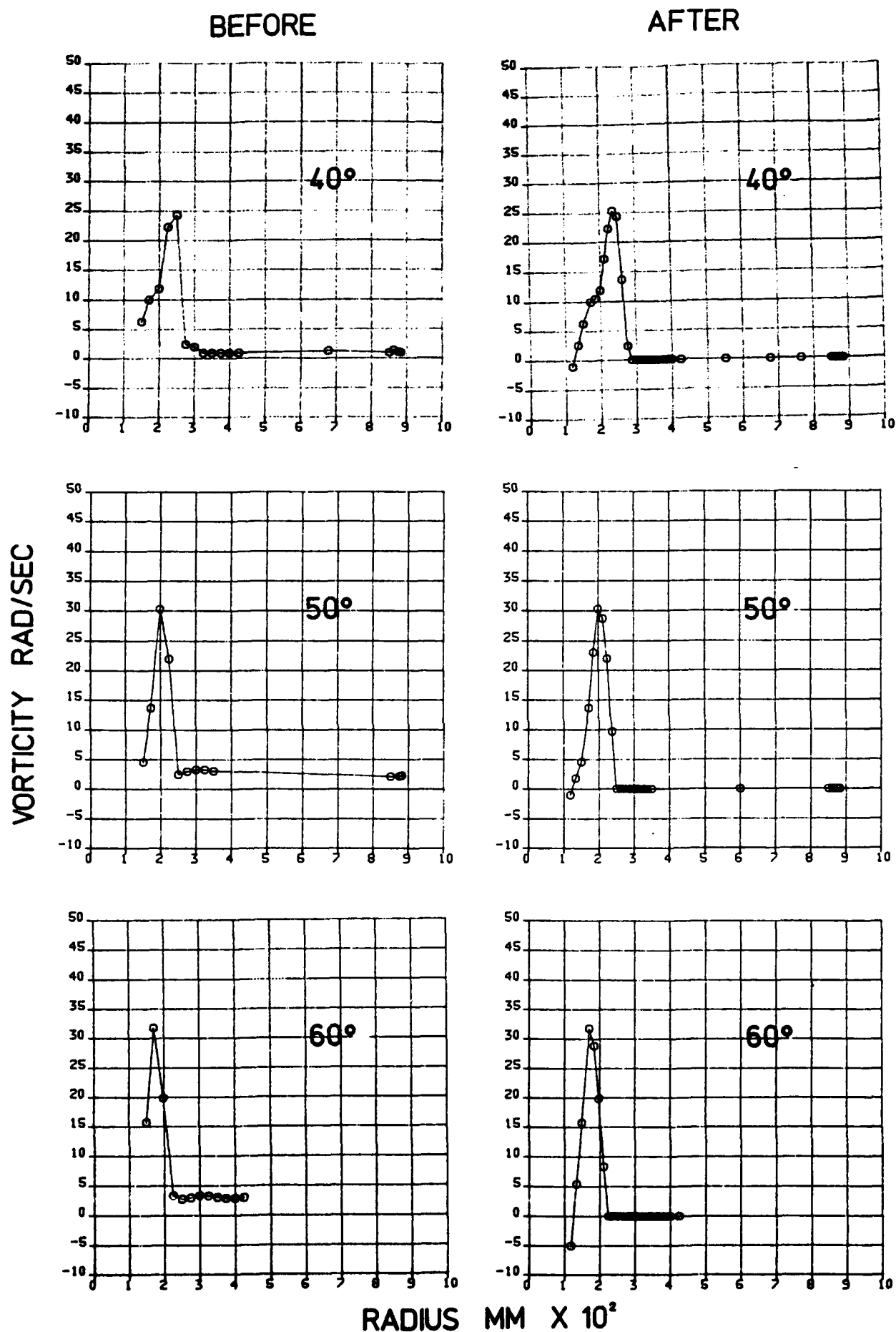


Figure 18b

VORTICITY TRAVERSES - BEFORE AND AFTER FAIRING
 ($x' = 0.925$, $r' = 0.3$, $\alpha = 7.5$)

BEFORE

AFTER

VORTICITY RAD/SEC

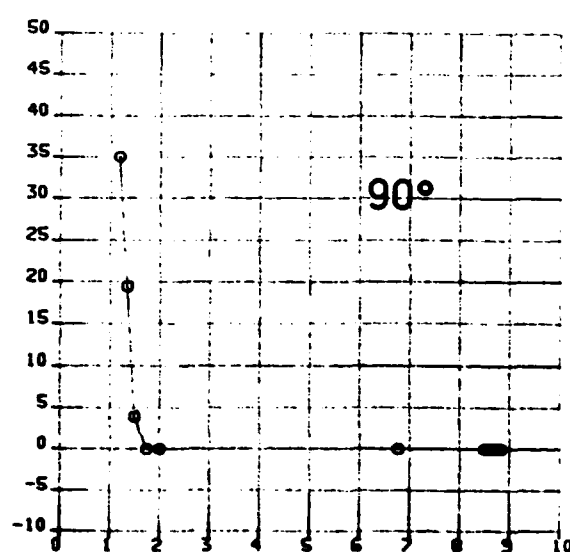
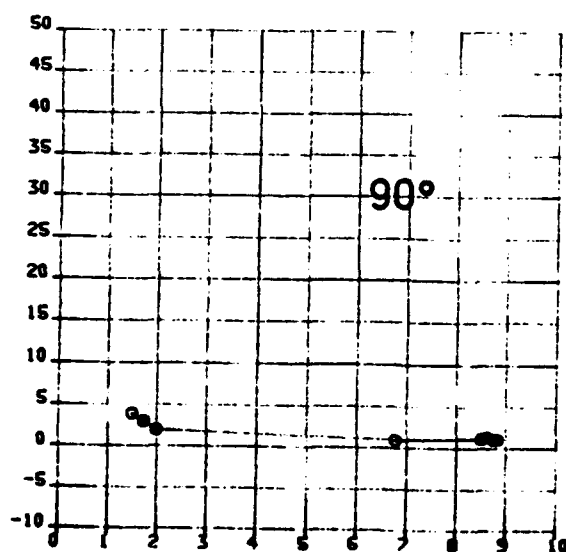
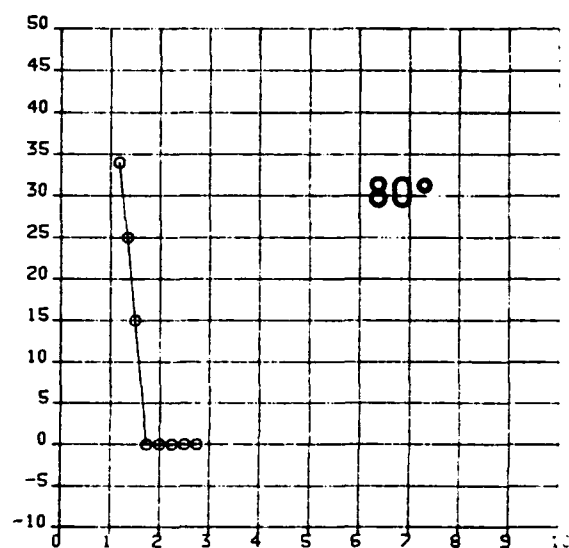
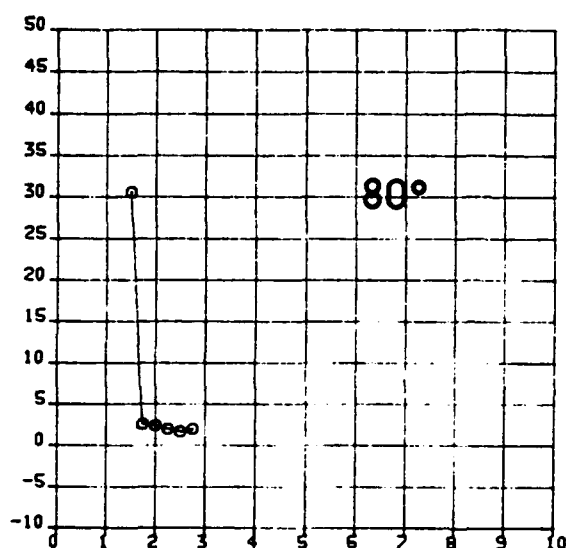
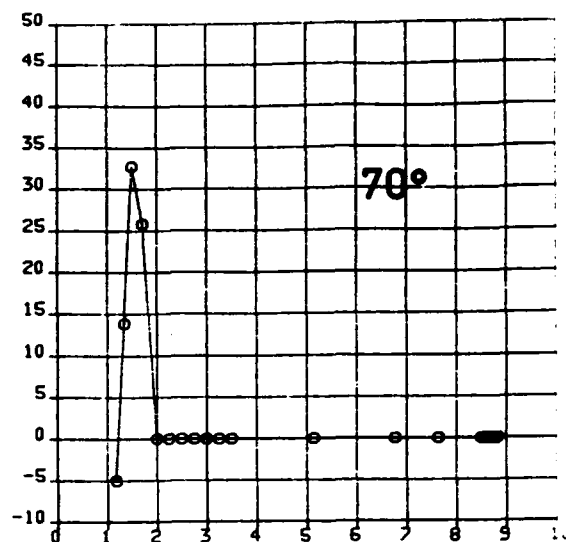
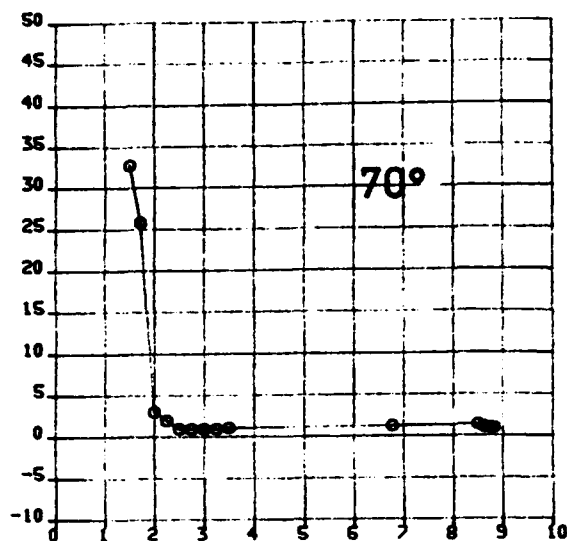
RADIUS MM $\times 10^2$

Figure 18c

VORTICITY TRAVERSES - BEFORE AND AFTER PAIRING

 $(x' = 0.925, r' = 0.3, \alpha = 7.5)$

values of θ often made reassessment of the position of the edge of the vortical flow necessary.

An artist's impression of the fairing of vorticity traverses can be seen in Figures 16 and 17. For further examples of the effects of fairing on traverses see Figures 18a to 18c.

5.6. Circulation

5.6.1. Local Circulation Density

In Figure 19 the circulation residing within a sector defined by the small angle $d\theta$ is

$$\Gamma_{\theta} d\theta = \int_0^{\infty} \zeta r dr d\theta \quad \text{m}^2/\text{sec}$$

and the local circulation density is

$$\Gamma_{\theta} = \int_0^{\infty} \zeta r dr \quad \text{m}^2/\text{sec}/\text{rad}$$

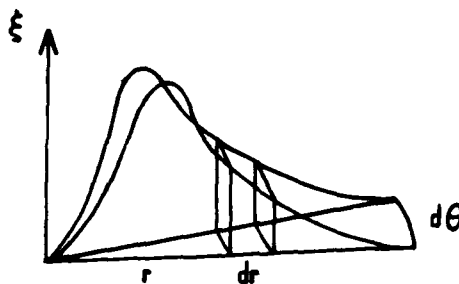


Figure 19

CIRCULATION IN A SECTOR

This local circulation density was calculated, like all other integrals in the analysis, using Trapezoidal rule.

Both negative and positive circulation densities were calculated. As a zero ζ -value was not always present in data where traverses cut the r -axis on the inboard side of the curve the method of 'regula falsi' was used to calculate the intersecting point as shown in Figure 20.

$$r_2 = r_1 - \frac{\zeta_1 (r_1 - r_0)}{\zeta_1 - \zeta_0}$$

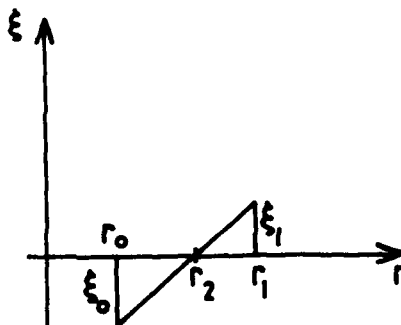


Figure 20

REGULA FALSI

A graph of the circulation density against angle was plotted for each experiment condition and an example is shown in Figure 21.

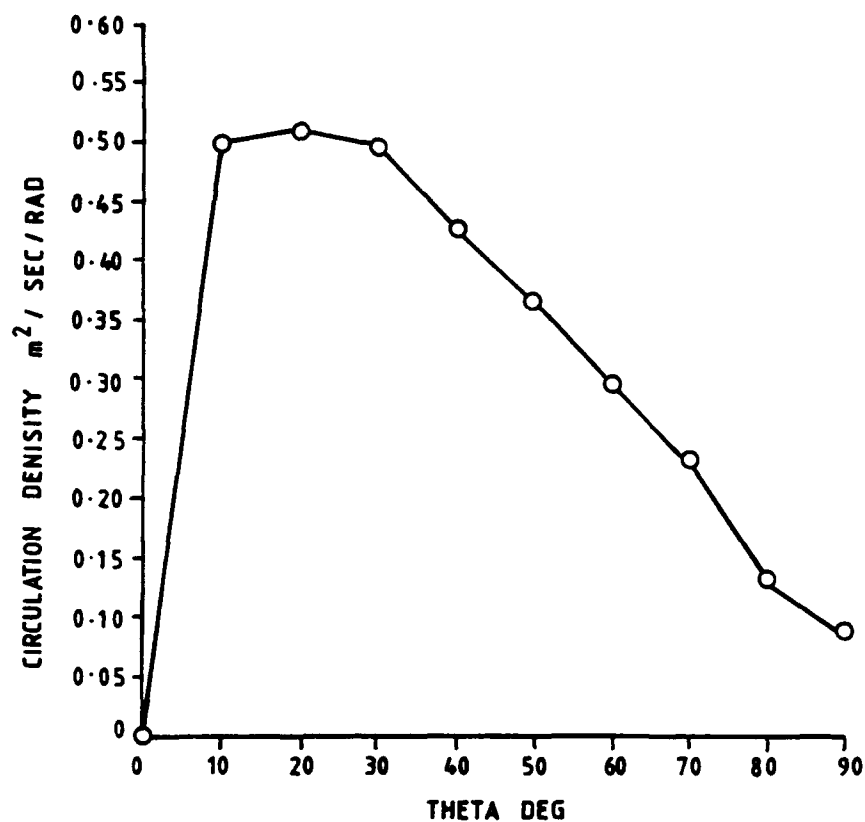


Figure 21

CIRCULATION DENSITY AGAINST STRUT ANGLE
($x' = 0.925$, $r' = 0.3$, $\alpha = 7.5$ DEGREES)

5.6.2. Total Circulation

The total circulation was estimated from

$$\Gamma = \int_0^{\pi/2} \Gamma_\theta d\theta \quad \text{m}^2/\text{sec}$$

Results for all test conditions at $x' = 0.925$ are shown in Figure 22.

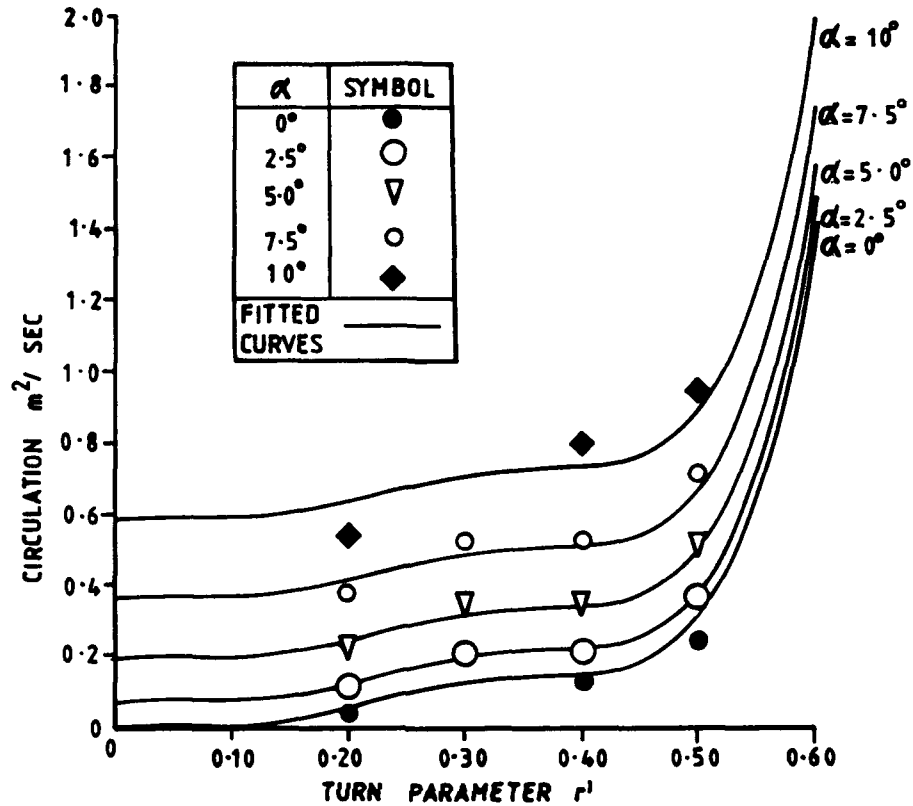


Figure 22

TOTAL CIRCULATION AGAINST TURN PARAMETER
FOR VARYING VALUES OF INCIDENCE ANGLE

5.7. Vortex Centres

5.7.1. Local Vortex Centre - Centre of Circulation Density

The radial location of the centre of the circulation density at a given angle θ is;

$$R_1 = \frac{\int_0^{\infty} \zeta r^2 dr}{\int_0^{\infty} \zeta r dr} \text{ metres}$$

(See Figures 19 and 23)

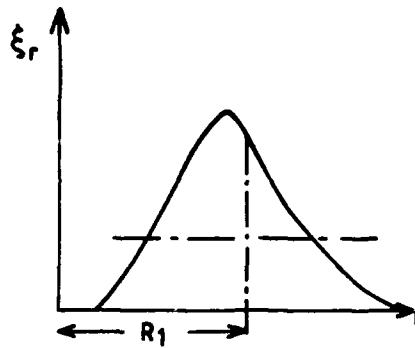


Figure 23

LOCAL VORTEX CENTRE

Values were calculated for all test conditions and an example is shown in Figure 24.

5.7.2. Total Vortex Centre - Centre of Total Circulation

The centre of the total circulation was calculated using the following integrals;

$$(R\theta)_{BV} = \frac{\int_0^{\infty} \int_0^{\pi/2} \zeta r^2 \theta d\theta dr}{\int_0^{\pi/2} \int_0^{\infty} \zeta r dr d\theta} \text{ metres.radians}$$

$$R_{BV} = \frac{\int_0^{\pi/2} \int_0^{\infty} \zeta r^2 dr d\theta}{\int_0^{\pi/2} \int_0^{\infty} \zeta r dr d\theta} \text{ metres (centre of circulation-radial position)}$$

$$\theta_{BV} = \frac{(R\theta)_{BV}}{R_{BV}} \text{ radians (centre of circulation-angular position)}$$

Results for all test conditions at $x' = 0.925$ are shown in Figures 25 and 26. (For convenience θ_{BV} is plotted in degrees).

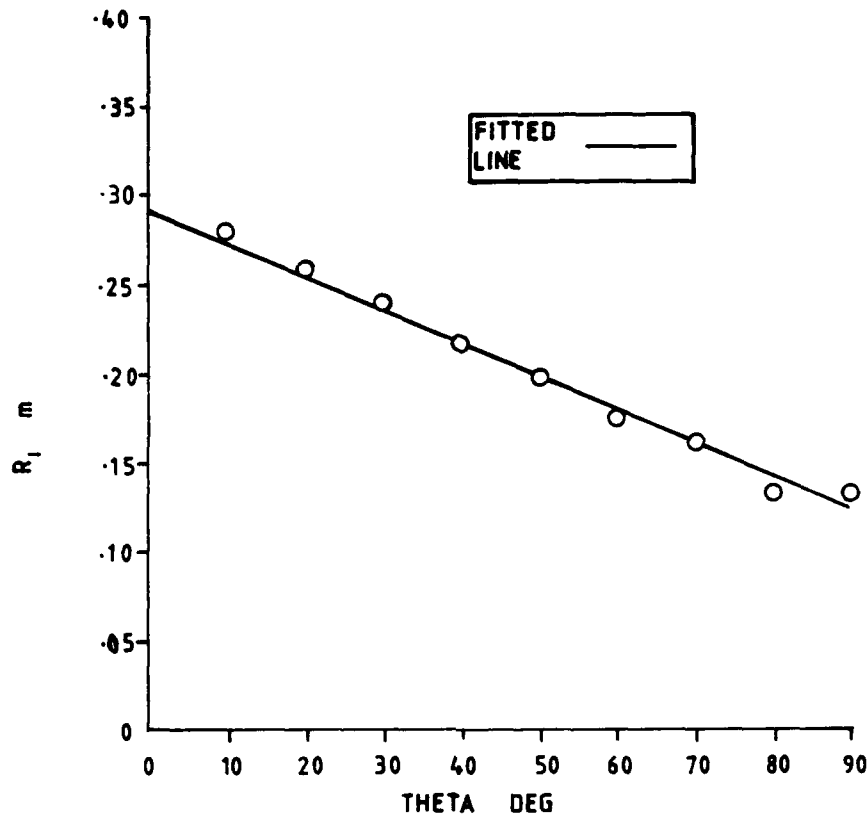


Figure 24

LOCAL VORTEX CENTRE AGAINST STRUT ANGLE
($x' = 0.925$, $r' = 0.2$, $\alpha = 7.5$ DEGREES)

5.8. Vortex Core Radius

According to Reference 6 the peak vorticity and the vortex core radius are related by the formula

$$\zeta_{\text{MAX}} = \frac{1.26 \Gamma}{\pi r_*^2} \quad \text{rad/sec}$$

Therefore

$$r_* = \sqrt{\frac{1.26 \Gamma_\theta}{\pi \zeta_{\text{MAX}}}} \quad \text{metres}$$

Figure 27 shows core radii calculated in this way for a particular test condition.

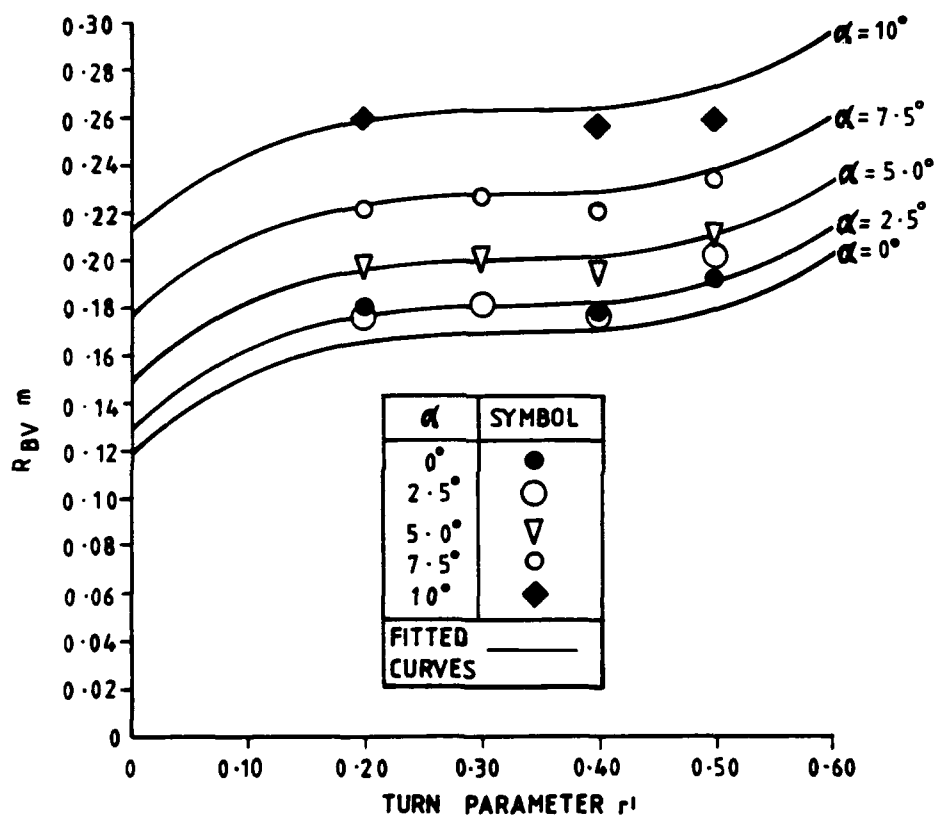


Figure 25

CENTRE OF CIRCULATION - RADIAL POSITION AGAINST
TURN PARAMETER FOR VARYING VALUES OF INCIDENCE ANGLE

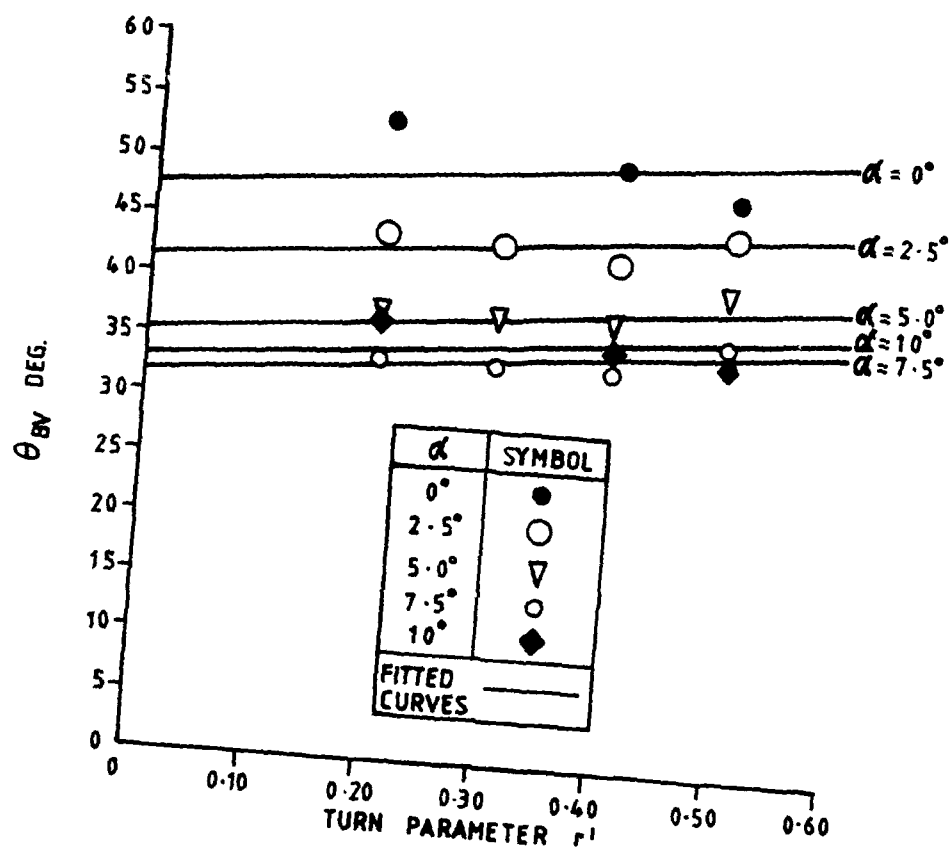


Figure 26

CENTRE OF CIRCULATION - ANGULAR POSITION AGAINST
TURN PARAMETER FOR VARYING VALUES OF INCIDENCE ANGLE

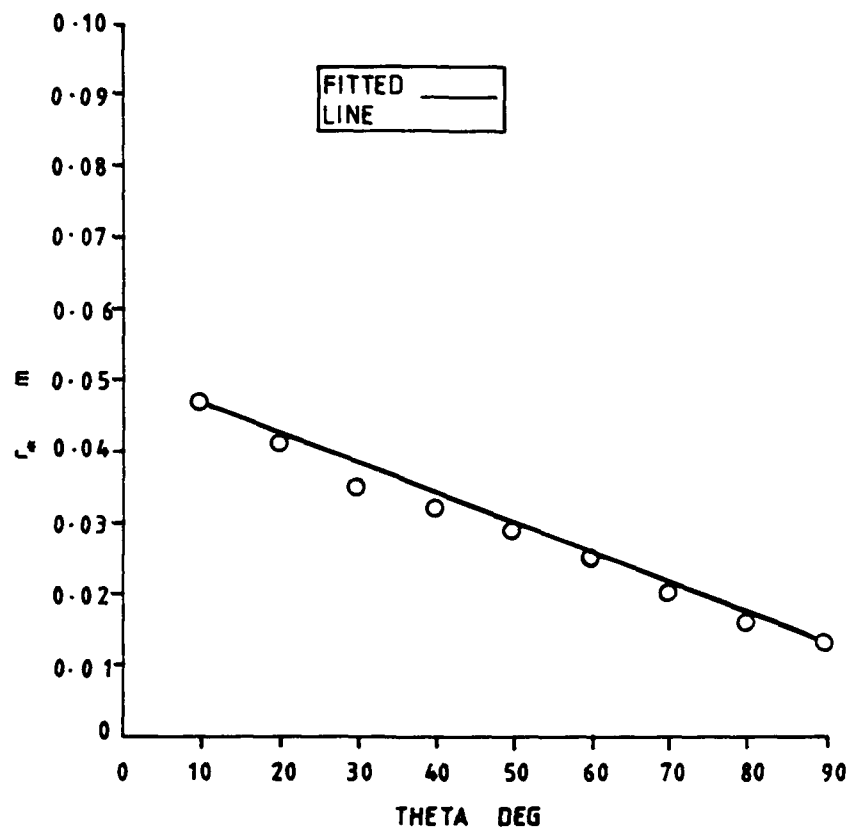


Figure 27

VORTEX CORE RADIUS AGAINST STRUT ANGLE
($x' = 0.925$, $r' = 0.3$, $\alpha = 2.5$ DEGREES)

6. EMPIRICAL EQUATIONS TO REPRESENT THE RESULTS

6.1. Circulation Density

Plots of circulation density against strut angle for varying test conditions were examined (see Figures 21 and 28). The trend of the plots suggested a sine curve would be appropriate with varying amplitude determined by the parameters r' , α and x' . The following equation was determined.

$$\Gamma_{\theta} = \left[c_2 r'^2 + c_1 r' + c_0 + \left[d_2 r'^2 + d_1 r' + d_0 \right] \alpha \right] \cdot \left[\sin \left[f_3 \theta^3 + f_2 \theta^2 + f_1 \theta \right] \right] \cdot \left[g_0 + g_1 x' \right] \quad (x' \geq 0.65) \text{ m}^2/\text{sec}/\text{rad}$$

$$\Gamma_{\theta} = 0 \quad (x' < 0.65)$$

(θ , α in degrees)

The coefficients of the above equation are noted in the following table.

c_2	c_1	c_0	d_2	d_1	d_0	f_3	f_2	f_1	g_0	g_1
-15.0	9.3	-1.4	2.0	-1.08	0.208	0.00012	-0.037	4.23	-2.398	3.66

NOTE:

$\Gamma_{\theta} = 0$ for all values of θ at $x' = 0.65$ where circulation becomes zero. The quality of the fit can be seen in the example shown in Figure 28.

6.2. Total Circulation

For $x' = 0.925$, plots were made of the circulation against turn parameter for each angle of incidence as shown in Figure 22.

The values appeared very consistent for 2.5 degrees, 5.0 degrees and 7.5 degrees angles of incidence. As data for 0 degrees and 10 degrees had come from the 1987 experiment when the probe was known to have been damaged, it was decided to base any further mathematical models largely on the trends of the three middle angles, but still taking 0 degrees and 10 degrees into account.

A regression polynomial of degree 5 with respect to r' fitted the data for $\alpha = 2.5$ degrees, 5.0 degrees, 7.5 degrees very well and the required behaviour as $r' \rightarrow 0$ was satisfied. The constant term of the polynomial was varied according to α .

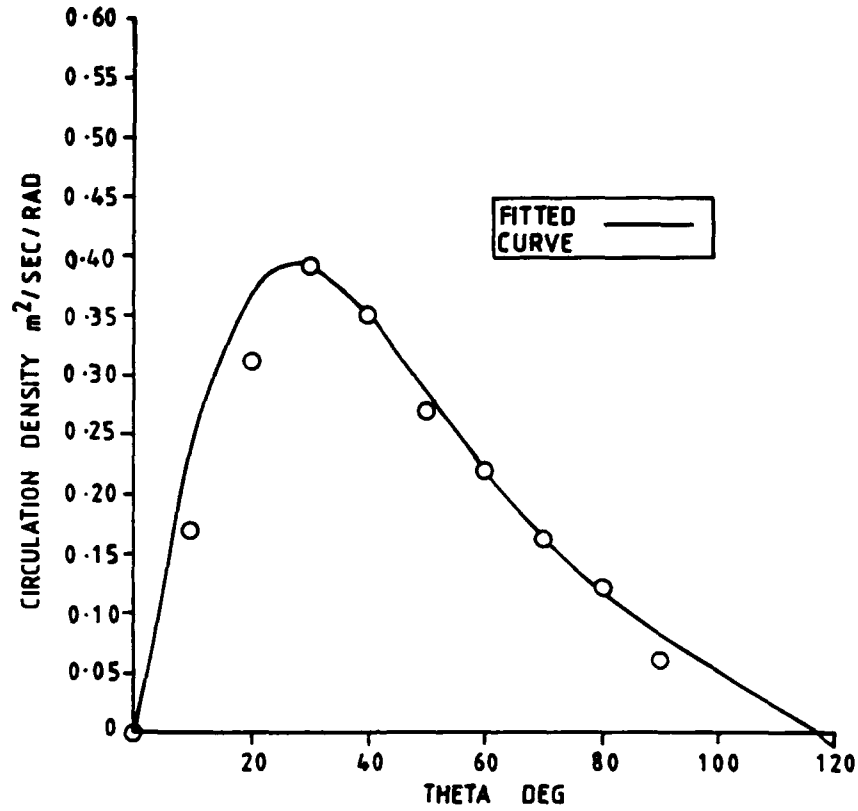


Figure 28

CIRCULATION DENSITY AGAINST STRUT ANGLE
($x' = 0.925$, $r' = 0.4$, $\alpha = 5$ DEGREES)

The equation for $x' = 0.925$ is as follows.

$$\Gamma_{(x'=0.925)} = h_5 r'^5 + h_4 r'^4 + h_3 r'^3 + h_2 r'^2 + h_1 r' + j_2 \alpha^2 + j_1 \alpha$$

$\text{m}^2/\text{sec} \quad (\alpha \text{ in degrees})$

A more general equation valid for all x' is as follows.

$$\Gamma = \begin{bmatrix} \Gamma_{(x'=0.925)} (k_1 x' + k_0) & (x' \geq 0.65) \\ 0 & (x' < 0.65) \end{bmatrix} \text{m}^2/\text{sec}$$

The coefficients of the above equations are noted in the following table.

h_5	h_4	h_3	h_2	h_1	j_2	j_1	k_1	k_0
258.78	-279.81	99.38	-11.81	0.48	0.004	0.018	3.67	-2.39

The quality of the fit of the equation at $x' = 0.925$ can be seen from Figure 22.

6.3. Local Vortex Centres

Plotting the local vortex centres radial position against strut angle for varying conditions it was immediately apparent (see Figure 24) that a linear equation was appropriate.

The following equation was derived.

$$R_1 = \begin{cases} (l_0 + l_1 \alpha + (m_0 + m_1 \alpha) r') \cdot (n_0 + n_1 x') \\ + ((p_0 + p_1 \alpha + (q_0 + q_1 \alpha) r') \theta) \cdot (s_0 + s_1 x') \\ + R & (x' \geq 0.65) \\ R & (x' < 0.65) \end{cases} \quad \text{metres}$$

(θ and α in degrees)

The coefficients of the above equation are noted in the following table.

l_0	l_1	m_0	m_1	n_0	n_1
30.864	15.97	212.89	- 12.4	- 0.00233	0.00359

p_0	p_1	q_0	q_1	s_0	s_1
- 0.344	- 0.165	- 1.857	0.0397	- 0.00229	0.00355

At $x' = 0.65$ where the circulation becomes zero the value of R_1 will equal the local body radius for all values of θ .

The quality of fit (see Figure 24) of the equation was consistently good for all test conditions with $x' = 0.925$.

6.4. Total Vortex Centre

The radial locations of the centre of circulation (for $x' = 0.925$) were plotted against turn parameter for each angle of incidence (Figure 25).

A regression polynomial of degree 3 was found to fit data for $\alpha = 2.5$ degrees, 5.0 degrees, 7.5 degrees with $x' = 0.925$ very well. The following equation was developed,

$$R_{BV}(x'=0.925) = t_3 r'^3 + t_2 r'^2 + t_1 r' + v_2 \alpha^2 + v_1 \alpha + 0.118 \quad \text{metres}$$

(α in degrees)

and more generally

$$R_{BV} = \left[\begin{array}{l} (\exp(z_3 x'^3 + z_2 x'^2 + z_1 x' + z_0) + W_0) \\ \cdot (t_3 r'^3 + t_2 r'^2 + t_1 r' + v_2 \alpha^2 + v_1 \alpha) \frac{R}{0.118} \\ + R \quad (x' \geq 0.65) \\ R \quad (x' < 0.65) \end{array} \right] \quad \text{metres}$$

(α in degrees)

The coefficients of the above equations are noted in the following table.

t_3	t_2	t_1	v_2	v_1
1.391	- 1.353	0.4492	0.00064	0.00296

z_3	z_2	z_1	z_0	W_0
5.06	- 8.0	5.62	- 1.67	- 0.993

Note that at $x' \approx 0.65$ the radial position is equal to the local radius of the body.

Likewise from plots of the θ position (for $x' = 0.925$) against turn parameter for each angle of incidence, (see Figure 26), the following linear equation was developed.

$$\theta_{BV}(x' = 0.925) = A_1 r' + B_3 \alpha^3 + B_2 \alpha^2 + B_1 \alpha + B_0 \quad \text{deg}$$

(α in degrees)

A general equation was developed.

$$\theta_{BV} = \left[\cos \left[F_2 x'^2 + F_1 x' + F_0 \right] + 1 \right] \cdot \left[A_1 r' + B_3 \alpha^3 + B_2 \alpha^2 + B_1 \alpha + B_0 \right] \text{ deg} \quad (x' > 0.65)$$

(α in degrees)

The coefficients of the above equations are noted in the following table.

A_1	B_3	B_2	B_1	B_0	F_2	F_1	F_0
7.76	0.024	-0.162	-2.25	47.68	6.724	-9.546	4.648

6.5. Vortex Core Radius

By calculating the core radius over angles 10 degrees to 90 degrees for all test conditions and by analysing the resulting values a linear equation appeared appropriate.

The following general equation was developed.

$$r_* = x' \left[G_0 + H_0 \alpha + J_0 \theta \right] \quad \text{metres} \quad (x' > 0.65)$$

(α, θ in degrees)

The coefficients of the above equation are noted in the following table.

G_0	H_0	J_0
0.0526	0.00095	-0.00046

The quality of the fit can be seen from Figure 27. It should be noted that the equation did not fit all the test condition data as well as that of the example but as mentioned previously not all the data can be considered very reliable. The above equation was derived from analysis of the most consistent data. Nevertheless the equation does reflect the linear trend and magnitude of most of the results.

7. CONCLUSIONS

Experiments on the Rotating Arm in the Manoeuvring Tank at ARE(H) provided data on vortices shed from a body of revolution in curved flow. The data contained apparent shortcomings as explained in this report. Methods as described above were used to fair the data to a

more expected form. The resulting faired data was used to develop empirical equations for local circulation density, total circulation density, apparent centre of total circulation, local vortex centre and local vortex core radius.

These expressions will be incorporated in the SUBSIM Computer program in due course.

REFERENCES

1. A R J M Lloyd. Progress Towards a Rational Method of Predicting Submarine Manoeuvres. RINA Symposium on Naval Submarines. London 1983.
2. Wolfson Unit for Marine Technology and Industrial Aerodynamics. Experiments on a Body of Revolution to Measure the Vortices Shed from the Body in Curved Flow. Report No 776. October 1986.
3. Wolfson Unit for Marine Technology and Industrial Aerodynamics. Experiments on a Body of Revolution to Measure the Vortices Shed from the Body in Curved Flow. Report No 807. April 1987.
4. A R J M Lloyd, I M C Campbell. Experiments to Investigate the Vortices Shed from a Submarine-Like Body of Revolution. Fifty-Ninth Meeting of the AGARD Fluid Dynamics Panel Symposium, Monterey, California, USA. Aerodynamics and Related Hydrodynamics Studies Using Water Facilities. AGARD-CPP 413. October 1986.
5. M M Freestone. Approximate Measurement of Streamwise Vorticity in Aeronautical Flows by a Simple Pressure Probe. I Mech E Symposium on Developments in Measurement and Instrumentation Engineering. Hatfield Polytechnic, September 1985.
6. A R J M Lloyd, P J Hanson. Decay of Trailing Vortices AMTE(H) R85213. October 1985. UNCLASSIFIED.

Document Control Sheet

(Notes on completion overleaf)

Overall security classification of sheet **UNCLASSIFIED**

(As far as possible this sheet should contain only unclassified information. If it is necessary to enter classified information, the box concerned must be marked to indicate the classification eg (R), (C) or (S)).

1. DRIC Reference (if known)		2. Originator's Reference ARE TM(UHU) 88305	
3. Agency Reference		4. Report Security Classification UNCLASSIFIED	
5. Originator's Code (if known)		6. Originator (Corporate Author) Name and Location	
5a. Sponsoring Agency's Code (if known)		6a. Sponsoring Agency (Contact Authority) Name and Location	
7. Title ANALYSIS OF EXPERIMENTS TO MEASURE BODY VORTICES IN CURVED FLOW			
7a. Title in Foreign Language (in the case of translations)			
7b. Presented at (for conference papers). Title, place and date of conference			
8. Author 1. Surname. Initials WARD B	9a. Author 2 LLOYD A R J M	9b. Authors 3,4..	10. Date pp ref 6.1988 35 6
11. Contract Number	12. Period	13. Project	14. Other References
15. Distribution Statement			
Descriptors (or keywords) BODY VORTICES MEASURED CURVED FLOW			
Abstract This Technical Memorandum describes the methods used to fair data on vortices shed from a body in curved flow. The methods used to calculate local circulation density, total circulation density, apparent centre of total circulation, local vortex centre and local vortex core radius are described and empirical equations to represent the results are given.			